Available online at www.sciencedirect.com

SciVerse ScienceDirect

Journal of the European Ceramic Society 32 (2012) 389–397

www.elsevier.com/locate/jeurceramsoc

Characterization of $Mg_xM_{2-x}P_2O_7$ (M = Cu and Ni) solid solutions

M.A. Tena *

Inorganic Chemistry Area, Inorganic and Organic Chemistry Department, Jaume I University, P.O. Box 224, Castellón, Spain

Received 5 September 2011; accepted 17 September 2011
Available online 12 October 2011

Abstract

In this study, $Mg_xM_{2-x}P_2O_7$ (M = Cu, Ni; $0 \le x \le 2$) and $Mg_{3-y}Ni_y(PO_4)_2$ ($0 \le y \le 3$) compositions were synthesized by the chemical coprecipitation method and characterized by X-ray diffraction, UV–vis–NIR spectroscopy and CIE L^* a^* b^* (Commission Internationale de l'Eclairage L^* a^* b^*) parameters measurements.

Solid solutions with α-$Cu_2P_2O_7$ and α-$Ni_2P_2O_7$ structures and solid solutions with $Ni_3(PO_4)_2$ structure were obtained from diphosphate and orthophosphate compositions respectively. Isostructurality of α-$Ni_2P_2O_7$ and α-$Mg_2P_2O_7$ structures enlarges the compositional range of solid solution formation respect to the $Mg_xCu_{2-x}P_2O_7$ solid solutions one.

The CIE L^* a^* b^* parameters in $Mg_xNi_{2-x}P_2O_7$ samples were obtained comparable with these parameters in others yellow materials suitable for ceramic pigments. $Mg_{0.5}Ni_{1.5}P_2O_7$ composition fired at 800 °C or 1000 °C is the optimal composition to obtain yellow materials with α-diphosphate structure in conditions of this study.

Keywords: Diphosphate; Orthophosphate; Solid solutions; Structure; Colour

1. Introduction

Most of divalent metal diphosphates, $M_2P_2O_7$, are polymorphic. Two crystalline forms are known for some $M_2P_2O_7$ (M = Mg(II), Mn(II), Fe(II), Ni(II), Cu(II) and Zn(II)): α-$M_2P_2O_7$ and β-$M_2P_2O_7$ (low and high temperature respectively).[1]

The α-$Cu_2P_2O_7$ has monoclinic symmetry with $a = 6.876(5)$ Å, $b = 8.113(5)$ Å, $c = 9.162(5)$ Å, $\beta = 109.54(6)°$, $Z = 4$ and space group $C2/c$.[2] The anion possesses a twofold axis and a P–O–P bond angle of 157°. The inner and outer P–O bonds of the anion are 1.58 and 1.53 Å respectively. A phase transformation is found to 373 K ($\alpha \rightarrow \beta$ transition). The structural data for β-$Cu_2P_2O_7$ at 100 °C are: $a = 6.827(8)$ Å, $b = 8.118(10)$ Å, $c = 4.576(6)$ Å, $\beta = 108.85(10)°$, space group $C2/m$ and $Z = 2$.[2]

α-$Ni_2P_2O_7$, the stable form at room temperature, is isostructural with the corresponding magnesium salt ($Mg_2P_2O_7$). Unit cell parameters $a = 13.093$ Å, $b = 8.275$ Å, $c = 8.974$ Å, $\beta = 104.94°$, space group $B2_1/c$ and $Z = 8$ have been reported for α-$Ni_2P_2O_7$ compound.[1] The lattice parameters of the α (low temperature) phase of $Mg_2P_2O_7$ are $a = 13.198(10)$ Å, $b = 8.295(5)$ Å, $c = 9.072(5)$ Å, $\beta = 104.9(1)°$ space group $B2_1/c$ and $Z = 8$.[3] The space group, $B2_1/c$, although non-primitive, allows an easy comparison of the α and β phases of $Mg_2P_2O_7$ compound.[3] A standard unit cell in space group $P2_1/c$ with $Z = 4$ could be chosen for α-modifications of $Ni_2P_2O_7$ and $Mg_2P_2O_7$ compounds.[4] Their $\alpha \rightarrow \beta$ transitions occur at 838 K and 343 K respectively.[1] β-$Ni_2P_2O_7$ and β-$Mg_2P_2O_7$ structures are isostructural with β-$Cu_2P_2O_7$. The structural data for β-$Ni_2P_2O_7$ are: $a = 6.501$ Å, $b = 8.239$ Å, $c = 4.480$ Å, $\beta = 104.14°$, space group $C2/m$ and $Z = 2$.[1] The structural data for β-$Mg_2P_2O_7$ are: $a = 6.494(7)$ Å, $b = 8.28(1)$ Å, $c = 4.522(5)$ Å, $\beta = 103.8(1)°$, space group $C2/m$ and $Z = 2$.[1]

In a structure, standard unit cell can be obtained from other unit cells by geometric transformations. The standard unit cell is the minimal part of a crystal which reproduces the structure by its repetition in the three directions. Its symmetry is in accordance with the standard conditions imposed by the operations of symmetry (standard settings) which are defined for each space group in International Tables of Crystallography. Table 1 shows main crystallographic data of diphosphates and orthophosphates of Cu, Ni and Mg obtained from Inorganic Crystal Structural Database (Standard cell).[4]

---

* Tel.: +34 964728249; fax: +34 964728214.
E-mail address: tena@qio.uji.es

0955-2219/$ – see front matter © 2011 Elsevier Ltd. All rights reserved.
doi:10.1016/j.jeurceramsoc.2011.09.018

Table 1
Structural information of Cu, Ni and Mg diphosphates and orthophosphates.

Structure	ICSD[a] reference	Crystalline system	Standard unit cell	Standard space group	*Z*
α-$Cu_2P_2O_7$	28279	Monoclinic	$a = 6.901$ Å, $b = 8.108$ Å, $c = 9.174$ Å, $\beta = 109.65$	$C12/c1$	4
α-$Ni_2P_2O_7$	27424	Monoclinic	$a = 6.935$ Å, $b = 8.267$ Å, $c = 8.970$ Å, $\beta = 113.74$	$P12_1/c1$	4
α-$Mg_2P_2O_7$	15326	Monoclinic	$a = 6.950$ Å, $b = 8.294$ Å, $c = 9.052$ Å, $\beta = 109.65$	$P12_1/c1$	4
β-$Cu_2P_2O_7$	27436	Monoclinic	$a = 6.827$ Å, $b = 8.118$ Å, $c = 4.576$ Å, $\beta = 108.85$	$C12/m1$	2
β-$Ni_2P_2O_7$	30433	Monoclinic	$a = 6.501$ Å, $b = 8.239$ Å, $c = 4.48$ Å, $\beta = 104.14$	$C12/m1$	2
β-$Mg_2P_2O_7$	20295	Monoclinic	$a = 6.49$ Å, $b = 8.28$ Å, $c = 4.51$ Å, $\beta = 104.08$	$C12/m1$	2
$Cu_3(PO_4)_2$	68811	Triclinic	$a = 4.848$ Å, $b = 5.280$ Å, $c = 6.183$ Å, $\alpha = 72.30$, $\beta = 86.90$, $\gamma = 68.59$	$P-1$	1
$Ni_3(PO_4)_2$	158523	Monoclinic	$a = 5.831$ Å, $b = 4.698$ Å, $c = 10.108$ Å, $\beta = 91.12$	$P12_1/c1$	2
$Mg_3(PO_4)_2$	9849	Monoclinic	$a = 5.911$ Å, $b = 4.734$ Å, $c = 10.214$ Å, $\beta = 90.99$	$P12_1/c1$	2
$Mg_3(PO_4)_2$	31005	Monoclinic	$a = 5.077$ Å, $b = 8.230$ Å, $c = 8.833$ Å, $\beta = 120.94$	$P12_1/c1$	2

[a] Inorganic crystal structure database.[4]

Aqueous precipitation route and hydrothermal synthesis are commonly used methods in synthesis of phosphates. The ceramic pigments industry tends towards cheap and simple processing. Cobalt ceramic dyes can be prepared by the chemical precipitation method.[5] The synthesis temperature in these ceramic dyes can be also reduced from phosphates precursors. From $NH_4H_2PO_4$ and $CoCO_3$ mixtures, crystallization of $Co_3(PO_4)_2$ occurs at about 625 °C. $Co_3(PO_4)_2$ and $Co_2P_2O_7$ structures introduce the Co^{2+} ions into glassy matrix. These structures are dissolved but ions remain in enamelled samples. The blue colour of enamelled samples is attributed to Co^{2+} ions.[5] Only cobalt violet phosphate and cobalt lithium phosphate are included in classification of the Mixed Metal Oxide Inorganic Coloured Pigments, DCMA.[6] No copper or nickel ceramic pigments with phosphate structure are included in it but solid solutions with diphosphate and orthophosphate structure might to be useful as precursors of ceramic dyes. P_2O_5 is included into the main glass-forming oxides together to SiO_2, B_2O_3 and GeO_2. Cations introduced from phosphates remain in glazed samples although a partial or total dissolution of these structures occurs. Thus, the introduction of chromophore cation in materials from phosphates might have some advantages in ceramic pigments industry.

In this study, the possible formation of $Mg_xM_{2-x}P_2O_7$ (M = Cu, Ni; $0 \le x \le 2$) solid solutions with a simple processing to apply in ceramic industry is investigated. The aim of this study is the structural characterization of these prepared materials in order to determine the compositional range for which these solid solutions with structure diphosphate develop blue and yellow colourations in enamelled samples. Chromatic coordinates in these diphosphate compositions are compared with orthophosphate samples when M = Ni.

2. Experimental procedures

$Mg_xM_{2-x}P_2O_7$ (M = Cu, Ni; $0 \le x \le 2$) and $Mg_{3-y}Ni_y(PO_4)_2$ ($0 \le y \le 3$) compositions were synthesized by the chemical coprecipitation method. The starting materials were $CuCl_2$ (Aldrich), $Ni(NO_3)_2 \cdot 6H_2O$ (Panreac), $MgCl_2 \cdot 6H_2O$ (Panreac), and H_3PO_4 (Sigma–Aldrich) of reagent grade chemical quality. A 0.5 M solution of H_3PO_4 in water was added on an aqueous solution of $MCl_2 \cdot xH_2O$ (M = Cu, Ni, Mg) with vigorous stirring at room temperature. After that, a solution of ammonium hydroxide was added dropwise until pH 8 and pH 10. The obtained precipitates were dried by an infrared lamp and dry samples were fired. When M = Cu, samples were fired between 300 and 800 °C for 5 days. $Mg_xNi_{2-x}P_2O_7$ compositions were fired between 300 and 1200 °C for 12 h and for 5 days.

A structure profile refinement was carried out by the Rietveld method (Fullprof.2k computer program).[7,8] Unit cell parameters and interatomic distances (M–O and P–O) in diphosphate and orthophosphate structures were obtained from $Mg_xM_{2-x}P_2O_7$ (M = Cu, Ni) and $Mg_{3-y}Ni_y(PO_4)_2$ fired compositions to investigate the possibility of formation of this solid solution in these synthesis conditions. The diffraction patterns were collected running between 5 and 110° 2θ, using monochromatic CuK_α radiation, a step size of 0.02° 2θ and a sampling time of 10 s. The initial structural information was obtained of the Inorganic Crystal Structure Database.[4] Table 1 includes the reference ICSD to every structure. This initial structural information also appears in Refs. [2,3] for the main structures of this study: α-$Cu_2P_2O_7$ and α-$Mg_2P_2O_7$.

UV–vis–NIR spectroscopy (diffuse reflectance) allows the Cu(II) and Ni(II) site in samples to be studied. A Jasco V-670 spectrophotometer was used to obtain the UV–vis–NIR (ultraviolet visible near infrared) spectra in the 200–2500 nm range. X-Rite spectrophotometer (SP60, an illuminant D65, an observer 10°, and a reference sample of MgO) was used to obtain CIE L^* a^* b^* colour parameters on fired samples and glazed tiles: L^* is the lightness axis (black (0) → white (100)), a^* the green (−) → red (+) axis, and b^* is the blue (−) → yellow (+) axis.[9]

In order to test their efficiency as ceramic pigment, the fired compositions were 4% weight enamelled with a commercial glaze (SiO_2–Al_2O_3–PbO–Na_2O–CaO glaze) onto commercial ceramic biscuits. Glazed tiles were fired for 5 min at 1065 °C and their UV–vis–NIR spectra and their CIE L^* a^* b^* colour parameters were obtained. These results were compared with the results obtained from powdered samples.

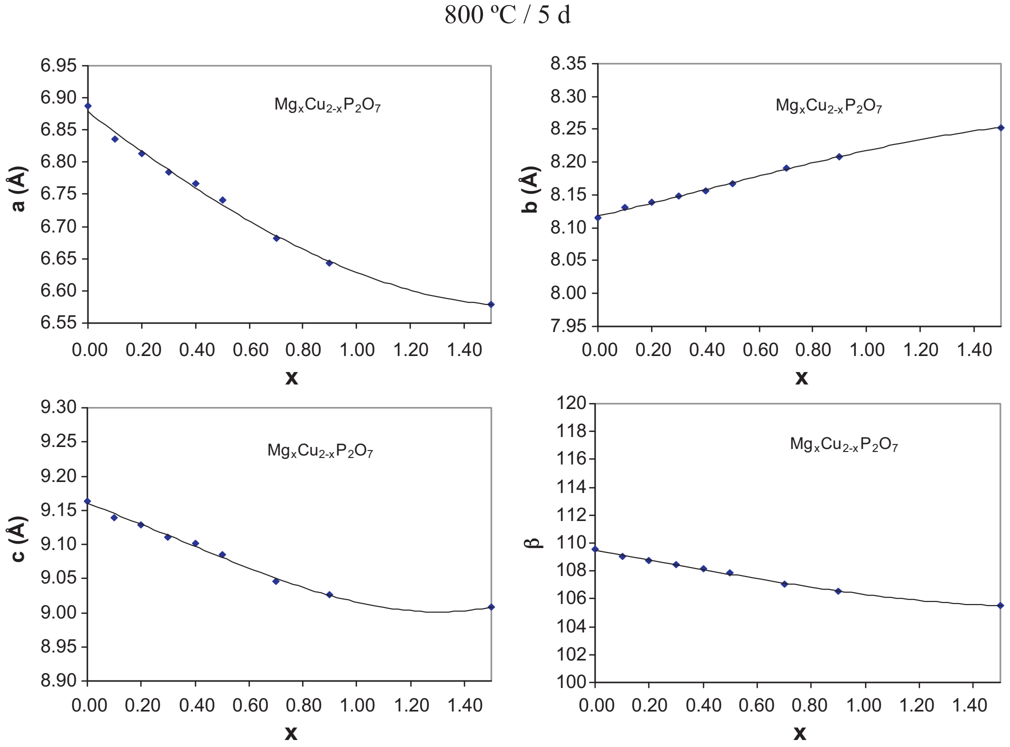

Fig. 1. Unit cell parameters in α-$Cu_2P_2O_7$ structure from $Mg_xCu_{2-x}P_2O_7$ ($0 \leq x \leq 1.5$) compositions fired at 800 °C/5 d.

3. Results and discussion

Table 2 shows crystalline phase evolution with composition and temperature in $Mg_xM_{2-x}P_2O_7$ (M = Cu, Ni; $0 \leq x \leq 2$) and $Mg_{3-y}Ni_y(PO_4)_2$ ($0 \leq y \leq 3$) samples. From samples fired at 300 °C, crystalline phases were not detected in conditions of this study. When diphosphate crystalline phase is detected in prepared samples, this phase is assignated to low temperature polimorph (α-$M_2P_2O_7$, M = Cu, Ni, Mg) although it is metastable at $T \geq 800$ °C.

When M = Cu, the major crystalline phase is α-$Cu_2P_2O_7$ in $Mg_xCu_{2-x}P_2O_7$ ($0 < x < 1$) compositions and α-$Mg_2P_2O_7$ in $Mg_xCu_{2-x}P_2O_7$ ($1 < x < 2$) compositions. $Cu_2P_2O_7$ and $Mg_2P_2O_7$ compounds have not the same structure. In α-$Cu_2P_2O_7$ with $C2/c$ space group, atoms or ions are in 8f general sites (Cu(II) ions (Cu1), phosphorus atoms (P1), oxygen atoms (three different crystallographic oxygen atoms: O2, O3, O4) and 4e special sites (central oxygen atom (O1) in $P_2O_7^{4-}$ groups). In α-$Mg_2P_2O_7$ with $P2_1/c$ space group, atoms or ions are all in 4e general sites (two different crystallographic Mg(II) ions (Mg1 and Mg2), two different crystallographic phosphorus atoms (P1, P2) and seven different crystallographic oxygen atoms (O1, O2, O3, O4, O5, O6, O7)). In $Mg_xCu_{2-x}P_2O_7$ compositions when $0 < x < 1$, Mg(II) and Cu(II) ions are in the same crystallographic site (atomic coordinates are the same). In these compositions (M = Cu), a small amount of $Cu_3(PO_4)_2$ is also present when

Table 2
Crystalline phases in $Mg_xM_{2-x}P_2O_7$ (M = Cu, Ni; $0 \leq x \leq 2$) and $Mg_{3-y}Ni_y(PO_4)_2$ ($0 \leq y \leq 3$) fired samples.

M	Nominal composition	Thermal history	Crystalline phases
Cu	$Mg_xCu_{2-x}P_2O_7$ ($0 \leq x \leq 0.9$)	800 °C/5 d	C(s), Cu(w)
Cu	$Mg_{1.5}Cu_{0.5}P_2O_7$ ($x = 1.5$)	800 °C/5 d	Ma(s), C(w), Mg(vw)
Cu	$Mg_2P_2O_7$ ($x = 2$)	800 °C/5 d	Ma(s)
Ni	$Mg_xNi_{2-x}P_2O_7$ ($0 \leq x \leq 1$)	800 °C/12 h	N(s)
Ni	$Mg_xNi_{2-x}P_2O_7$ ($1 < x \leq 2$)	800 °C/12 h	Ma(s)
Ni	$Mg_xNi_{2-x}P_2O_7$ ($0 \leq x \leq 1$)	1000 °C/12 h	N(s)
Ni	$Mg_xNi_{2-x}P_2O_7$ ($1 < x \leq 2$)	1000 °C/12 h	Ma(s)
Ni	$Mg_xNi_{2-x}P_2O_7$ ($0 \leq x \leq 0.5$)	1200 °C/5 d	N(s), Ni(m)
Ni	$Mg_3(PO_4)_2$ ($y = 0$)	800 °C/12 h	Mg(s)
Ni	$Mg_2Ni(PO_4)_2$ ($y = 1$)	800 °C/12 h	Mg(s), Ni(w)
Ni	$MgNi_2(PO_4)_2$ ($y = 2$)	800 °C/12 h	Ni(s)
Ni	$Ni_3(PO_4)_2$ ($y = 3$)	800 °C/12 h	Ni(s)

Crystalline phases: (Mg, M)$_2P_2O_7$ ss (M = Cu, Ni) with α-$M_2P_2O_7$ structure and $M_2P_2O_7$-rich composition, C = α-$Cu_2P_2O_7$, N = α-$Ni_2P_2O_7$ and Ma = α-$Mg_2P_2O_7$. N and Ma present the same structure. (Mg, M)$_3(PO_4)_2$ ss (M = Cu, Ni) with $M_3(PO_4)_2$ structure, Cu = $Cu_3(PO_4)_2$, Ni = $Ni_3(PO_4)_2$ and $Mg_3(PO_4)_2$ ($\beta = 90.99$), Mg = $Mg_3(PO_4)_2$ ($\beta = 120.94$) [ss: solid solutions]. Diffraction peak intensity: s = strong, m = medium, w = weak, vw = very weak.

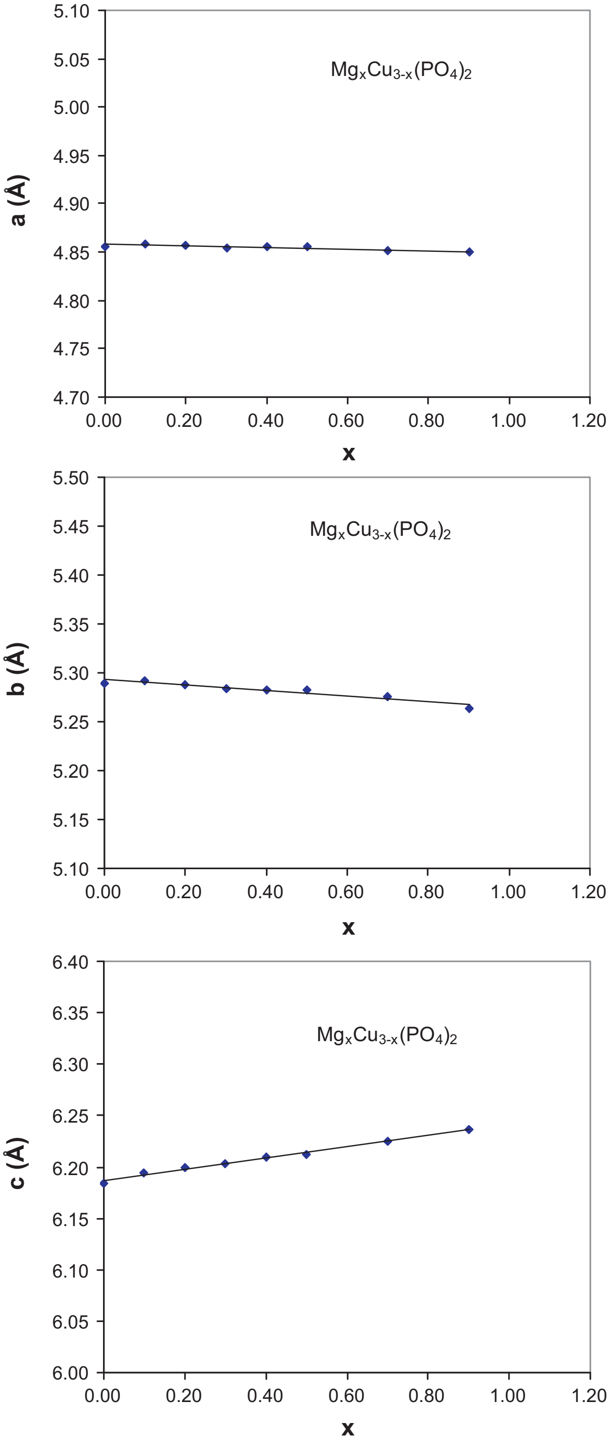

Fig. 2. Unit cell parameters in $Cu_3(PO_4)_2$ structure from $Mg_xCu_{2-x}P_2O_7$ $(0 \leq x < 1)$ compositions fired at 800 °C/5 d.

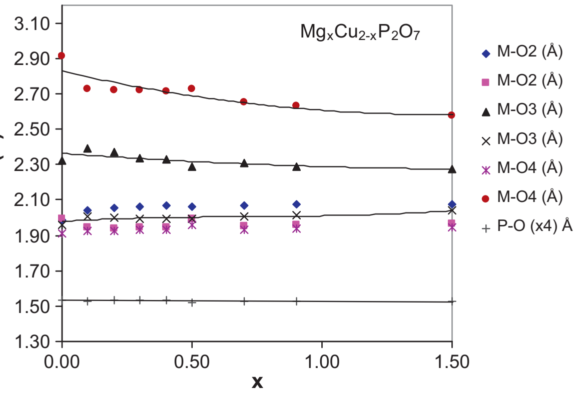

Fig. 3. Interatomic distances less than 3 Å to M (Cu, Mg) and P atoms for α-$Cu_2P_2O_7$ structure in $Mg_xCu_{2-x}P_2O_7$ $(0 \leq x \leq 1.5)$ compositions fired at 800 °C/5 d.

$0 \leq x \leq 0.9$. This orthophosphate crystalline phase ($Cu_3(PO_4)_2$) is present with triclinic symmetry and $P-1$ space group. Cu(II) ions are in 1a special sites (Cu1) and 2i general sites (Cu2), phosphorus atoms (P1) and oxygen atoms (O1, O2, O3, O4) are also in 2i sites in this structure.

α-Diphosphate crystalline phase is detected as a only crystalline phase in $Mg_xNi_{2-x}P_2O_7$ $(0 \leq x \leq 2)$ samples fired at 800 °C and 1000 °C, but this phase is detected together with orthophosphate one at 1200 °C. $Ni_2P_2O_7$, $Mg_2P_2O_7$ and $Mg_xNi_{2-x}P_2O_7$ compositions are detected with the same α-$Mg_2P_2O_7$ structure above described with all ions and atoms in 4e sites. In $Mg_xNi_{2-x}P_2O_7$ $(0 < x < 2)$ compositions, Mg(II) and Ni(II) coordinates are the same and these coordinates change slightly with composition (x).

Orthophosphate crystalline phases ($M_3(PO_4)_2$) are detected from $Mg_{3-y}Ni_y(PO_4)_2$ $(0 \leq y \leq 3)$ compositions fired at 800 °C. The main differences in $Ni_3(PO_4)_2$ (ICSD-158523) and $Mg_3(PO_4)_2$ (ICSD-9849 and ICSD-31005) crystalline phases are the b parameter and the β angle (Table 1). When $0 \leq y \leq 1$, the $Mg_3(PO_4)_2$ crystalline phase (ICSD-31005) is present in the samples and when $2 \leq y \leq 3$, the $Ni_3(PO_4)_2$ crystalline phase (ICSD-158523 and ICSD-9849) is obtained from the samples. $Mg_3(PO_4)_2$ and $Ni_3(PO_4)_2$ orthophosphate crystalline phases are detected with monoclinic symmetry with $P2_1/c$ space group (Table 1). Ni(II) and Mg(II) ions are in 2a special sites (Ni1, Mg1) and 4e general sites (Ni2, Mg2) in this space group and phosphorus atoms (P1) and oxygen atoms (O1, O2, O3, O4) are also in 4e sites in it.

In the conditions of this study, changes in development of crystalline phases are not observed from samples precipitated until pH 8 or pH 10 in synthesis. Stoichiometric ratio of raw materials is the main variable to obtain these studied diphosphates.

Figs. 1 and 2 show the α-diphosphate and orthophosphate unit cell parameters for prepared samples when M = Cu. The variation of these parameters with composition confirms the formation of α-$Cu_2P_2O_7$ solid solutions and $Cu_3(PO_4)_2$ solid solutions.

At 800 °C in α-$Cu_2P_2O_7$ structure, a and c unit cell parameters decrease slightly according with the replacement of Cu(II) ion by a slightly smaller one (Mg(II)) from $Mg_xCu_{2-x}P_2O_7$ compositions when $0 \leq x \leq 0.9$. An increase in b unit cell parameter is detected (Fig. 1) from these compositions. This fact cannot be explained from ionic radii values. A slight contract of unit cell is expected. Structural distortion might explain the b increase with incorporation of Mg(II) ions in the α-$Cu_2P_2O_7$ structure.

Fig. 3 shows interatomic distances less than 3 Å to M (Cu, Mg) and P atoms for α-$Cu_2P_2O_7$ structure in $Mg_xCu_{2-x}P_2O_7$

($0 \le x \le 1.5$) samples. Significant changes in the M–O distances for the nearest to M (Cu, Mg) four oxygen are not detected. The distances M-O3 and M-O4 decrease with x. The decrease of these M–O distances less than 3 Å might explain structural distortion and lost of stability of α-$Cu_2P_2O_7$ structure at high x values. α-$Cu_2P_2O_7$ structure is a layered structure where diphosphate groups (two tetrahedral shared O1) are linking the layers. In this structure cation coordination is 5 (Cu1). α-$Mg_2P_2O_7$ structure with three-dimensional character is a more rigid structure than α-$Cu_2P_2O_7$ one. Cation coordination is 5 (Mg1) and 6 (Mg2) in it. From $x = 0$ ($Cu_2P_2O_7$) and $x = 2$ ($Mg_2P_2O_7$) compositions, experimental results in this study are in accordance with structural data in Inorganic Crystal Structure Database (α-diphosphate polymorph with ICSD-28279 and ICSD-15326 respectively).

Variation of unit cell parameters in $Cu_3(PO_4)_2$ structure (shown in Fig. 2) indicates the formation of solid solutions in this structure when this phase is present in prepared samples. The c unit cell parameter increases with x according with the different value of this parameter in $Cu_3(PO_4)_2$ and $Mg_3(PO_4)_2$ structures. In $Cu_3(PO_4)_2$ structure (ICSD-68811) cation coordination is 4 (Cu1) and 5 (Cu2). In $Mg_3(PO_4)_2$ structure (ICSD-31005) cation coordination is 5 (Mg1) and 6 (Mg2) and in $Mg_3(PO_4)_2$ structure (ICSD-9849) cation coordination is 6 (Mg1) and 6 (Mg2). These values are in accordance with interatomic distances obtained in this study in $Cu_3(PO_4)_2$ structure from $Mg_xCu_{2-x}P_2O_7$ compositions. $Mg_3(PO_4)_2$ structure is not detected from them. Interatomic distances in $Cu_3(PO_4)_2$ structure obtained from $Mg_xCu_{2-x}P_2O_7$ ($0 \le x \le 0.9$) compositions are similar (Fig. 4). Structural distortion is not observed in this structure.

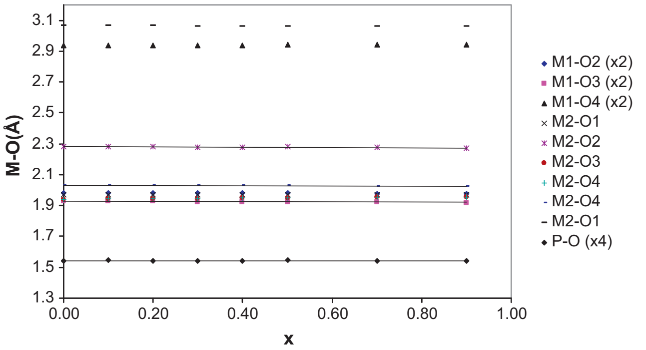

Fig. 4. M–O and P–O interatomic distances less than 3.2 Å for $Cu_3(PO_4)_2$ structure in $Mg_xCu_{2-x}P_2O_7$ ($0 \le x < 1$) compositions fired at 800 °C/5 d.

Fig. 5 shows the α-$Ni_2P_2O_7$ unit cell parameters for $Mg_xNi_{2-x}P_2O_7$ ($0 \le x \le 2$) samples fired at 800 °C, 1000 °C and 1200 °C. The variation of these parameters with composition confirms the formation of prepared solid solutions with α-$Ni_2P_2O_7$ structure. Unit cell parameters obtained in α-$Ni_2P_2O_7$ structure for these compositions are in accordance with an expansion of unit cell when x increases. This increase is due to the replacement of Ni(II) ion by a slightly greater one (Mg(II)).

Because of the α-$Ni_2P_2O_7$ structure is the same than α-$Mg_2P_2O_7$ one, the α-$M_2P_2O_7$ (M = Ni, Mg) solid solutions are formed in all compositional range between $Ni_2P_2O_7$ and $Mg_2P_2O_7$ compounds. Linear variation of unit cell parameters (Vegard's law behaviour) is observed in these compositions. It indicates that these solid solutions are formed by random substitution or distribution of ions. In this case ($Mg_xNi_{2-x}P_2O_7$ ($0 \le x \le 2$) samples) the changes in unit cell parameters with composition are governed purely by the relative sizes of the atoms or ions in solid solutions (Ni(II) and Mg(II) ions).

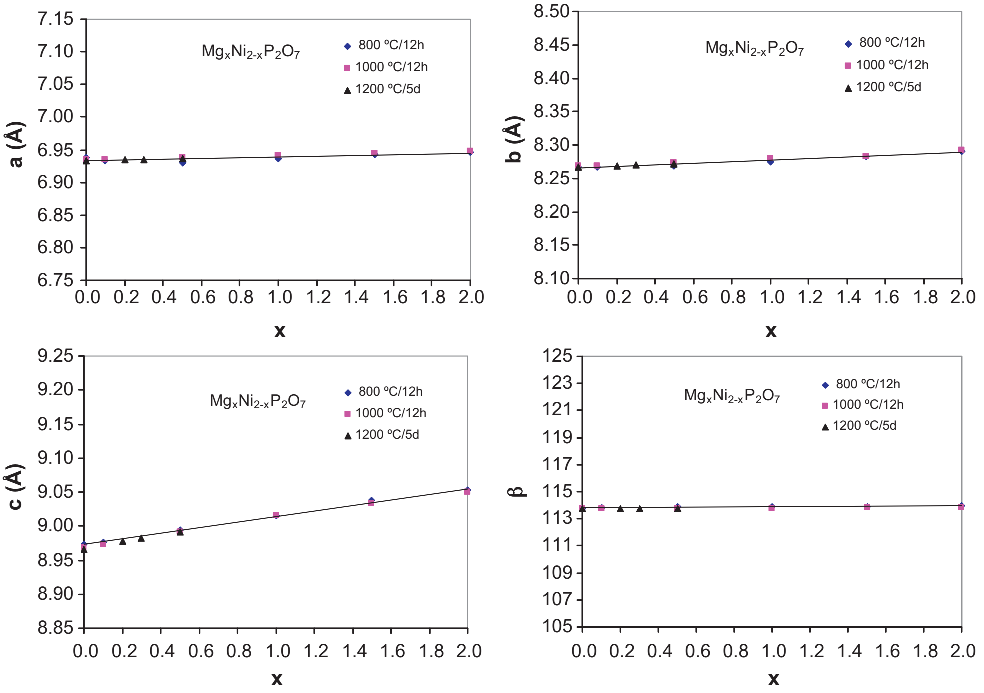

Fig. 5. Unit cell parameters in α-$Ni_2P_2O_7$ structure in $Mg_xNi_{2-x}P_2O_7$ ($0 \le x < 2$) compositions fired at 800 °C/12 h, 1000 °C/12 h and 1200 °C/5 d.

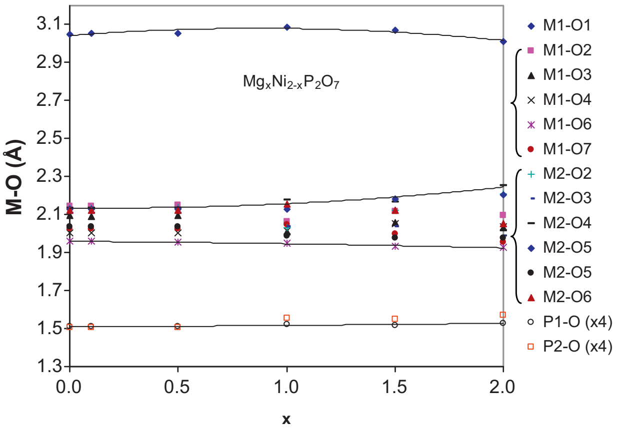

Fig. 6. M–O (M = Ni, Mg) and P–O interatomic distances less than 3.2 Å in $Mg_xNi_{2-x}P_2O_7$ ($0 \leq x \leq 2$) compositions fired at 800 °C/12 h with α-$Ni_2P_2O_7$ structure.

M–O (M = Ni, Mg) and P–O interatomic distances less than 3.2 Å in $Mg_xNi_{2-x}P_2O_7$ ($0 \leq x \leq 2$) compositions fired at 800 °C with α-$Ni_2P_2O_7$ structure are shown in Fig. 6. Differences in interatomic M–O distances are detected smaller when M = Ni than when M = Mg. Significative change in M–O distances out of first coordination of Ni(II) or Mg(II) ions is not observed. This fact is in accordance with stability of this α-$M_2P_2O_7$ (M = Ni, Mg) structure in all the compositional range between $Ni_2P_2O_7$ and $Mg_2P_2O_7$ compounds ($0 \leq x \leq 2$) at 800 and 1000 °C. In these solid solutions the cation coordination obtained is 5 equal than in α-$Ni_2P_2O_7$ (ICSD-27424) and α-$Mg_2P_2O_7$ structures (ICSD-15326). The cation coordination is 5 (Ni1 and Mg1) and 6 (Ni2 and Mg2) in them.

From these results, it might be established the compositional range for which the α-$M_2P_2O_7$ (M = Cu, Ni) structures are maintained at 800 °C in $Mg_xM_{2-x}P_2O_7$ (M = Cu, Ni) solid solutions. At this temperature, it is $0 \leq x \leq 0.8$ when M = Cu and it is $0 \leq x \leq 2$ when M = Ni.

Fig. 7 shows the unit cell parameters in $Ni_3(PO_4)_2$ structure obtained for $Mg_{3-y}Ni_y(PO_4)_2$ samples fired at 800 °C/12 h. The variation of these parameters with composition indicates the formation of solid solutions with $Ni_3(PO_4)_2$ structure when $1 \leq y \leq 3$. Unit cell parameters obtained from $Mg_{3-y}Ni_y(PO_4)_2$ samples are in accordance with a contraction of unit cell when y increases (Mg(II) ion is slightly greater than Ni(II)). In these solid solutions with $Ni_3(PO_4)_2$ structure (ICSD-158523, ICSD-9849) cation coordination is 6 (Ni1, Ni2, Mg1, Mg2).

UV–vis–NIR spectra of $Mg_xCu_{2-x}P_2O_7$ ($0 < x < 1.5$) samples fired at 800 °C are shown in Fig. 8. No appreciable changes of coordination of Cu(II) ion with composition are detected from UV–vis–NIR spectra. This is in accordance with results obtained from XRD. First coordination of Cu(II) ion does not change when these solid solutions are formed (significant changes in the four smallest distances M–O (M = Cu, Mg) from $Mg_xCu_{2-x}P_2O_7$ ($0 < x < 1.5$) solid solutions with α-$Cu_2P_2O_7$ structure are not detected). Spectra show a strong absorbance in 700–1400 nm wavelength range with the absorption maximum at ≈850 nm. Most of complex with Cu(II) ion are formed with four ligands (IC = 4). The reason for the inusual behaviour is

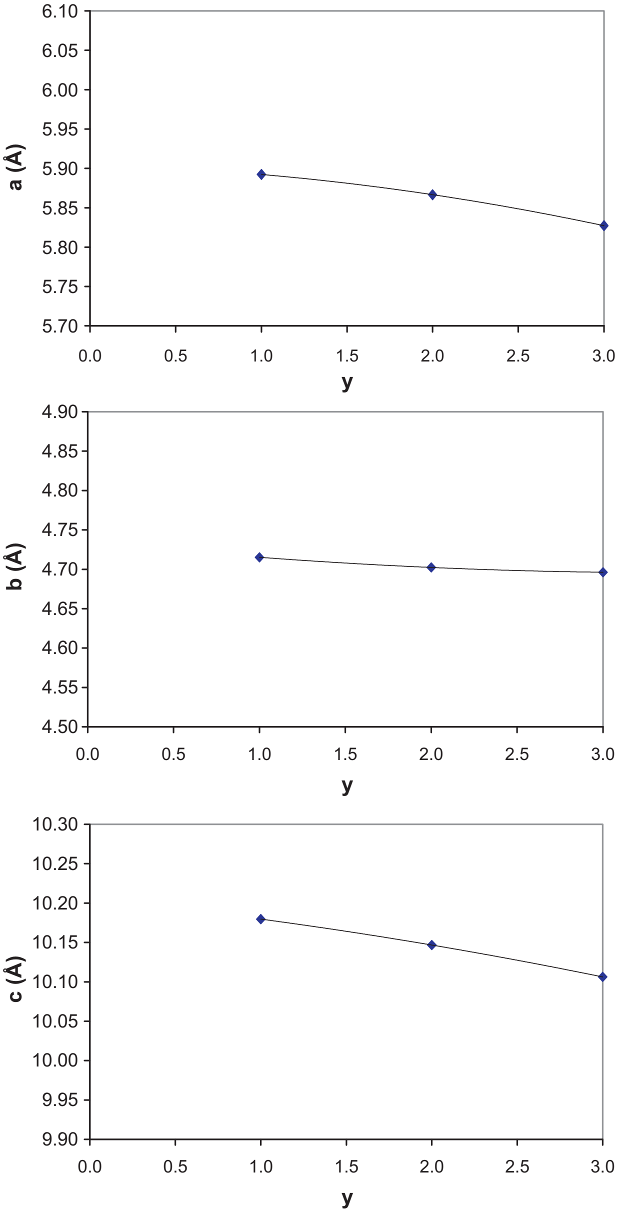

Fig. 7. $Ni_3(PO_4)_2$ unit cell parameters from $Mg_{3-y}Ni_y(PO_4)_2$ ($1 \leq y \leq 3$) samples fired at 800 °C/12 h.

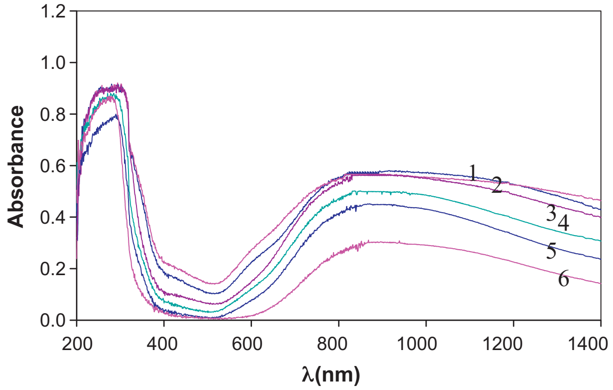

Fig. 8. UV–vis–NIR spectra of $Mg_xCu_{2-x}P_2O_7$ samples fired at 800 °C with $x = 0.0$ (1), $x = 0.1$ (2), $x = 0.4$ (3), $x = 0.7$ (4), $x = 1.0$ (5), $x = 1.5$ (6).

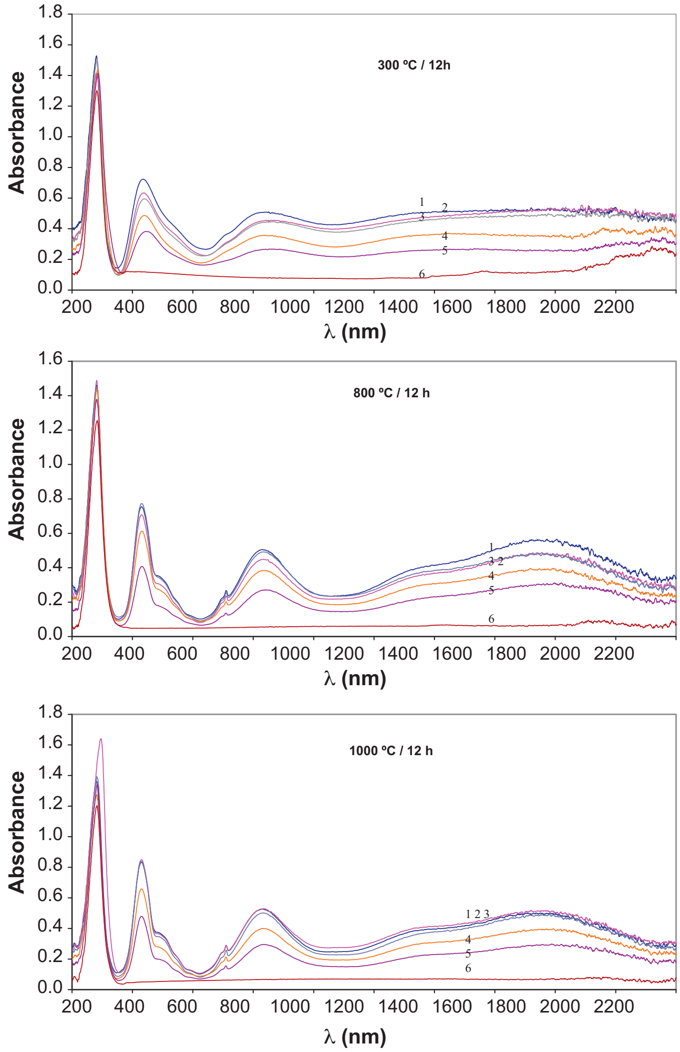

Fig. 9. UV–vis–NIR spectra of $Mg_xNi_{2-x}P_2O_7$ samples fired at 300 °C/12 h, 800 °C/12 h and 1000 °C/12 h with $x = 0.0$ (1), $x = 0.1$ (2), $x = 0.5$ (3), $x = 1.0$ (4), $x = 1.5$ (5), $x = 2.0$ (6).

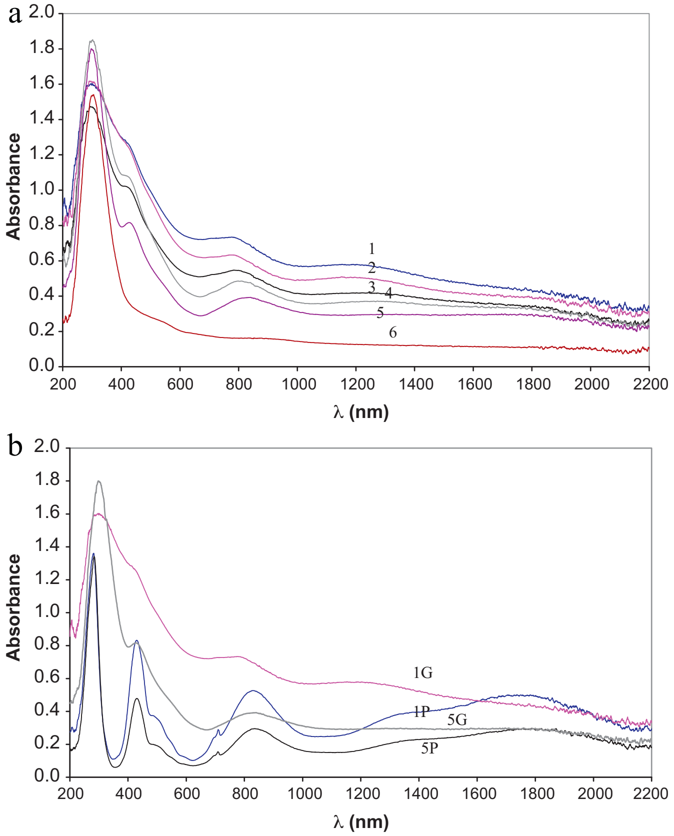

Fig. 10. UV–vis–NIR spectra of $Mg_xNi_{2-x}P_2O_7$ samples fired at 1000 °C: (a) from glazed tiles with $x = 0.0$ (1), $x = 0.1$ (2), $x = 0.5$ (3), $x = 1.0$ (4), $x = 1.5$ (5), $x = 2.0$ (6); (b) from glazed tiles with $x = 0.0$ (1G), $x = 1.5$ (5G) and from powdered samples with $x = 0.0$ (1P), $x = 1.5$ (5P).

connected with the Jahn–Teller effect. Because of it, the Cu(II) ions does not bind the fifth and sixth ligands strongly. In the aqua, the absorption maximum of this ion is at ≈800 nm, similar ligand field than in diphosphate structure. This fact is in accordance with weak blue colouration (greenish-blue colour) of samples (Table 3). Small b^* (−) values are obtained. The absorption spectra obtained from glazed tiles are similar than these obtained from powdered samples and it is the same for all compositions.

Table 3
CIE $L^*a^*b^*$ parameters in $Mg_xCu_{2-x}P_2O_7$ ($0 < x < 2$) samples fired at 800 °C/5 d.

x	L^*	a^*	b^*
0.1	78.01	−18.20	−3.92
0.2	81.41	−15.28	−3.28
0.3	81.89	−14.57	−3.65
0.4	84.58	−12.63	−2.50
0.5	85.06	−12.09	−2.47
0.7	85.39	−12.16	−4.02
0.9	88.22	−10.00	−3.37
1.5	91.30	−4.65	0.21

Fig. 9 shows the UV–vis–NIR spectra in $Mg_xNi_{2-x}P_2O_7$ ($0 \le x \le 2$) fired samples. Absorption bands detected can be assigned to Ni^{2+} in an octahedral site. The three spin allowed transitions: $^3A_{2g} \rightarrow {}^3T_{2g}(F)$, $^3A_{2g} \rightarrow {}^3T_{1g}(F)$ and $^3A_{2g} \rightarrow {}^3T_{1g}(P)$ generally fall within the ranges 1400–800, 900–500 and 550–370 nm respectively in octahedral system.[10] Detected bands at 400–550, 750–950 and 1250–1450 nm are due at third ($^3A_{2g} \rightarrow {}^3T_{1g}(P)$), second ($^3A_{2g} \rightarrow {}^3T_{1g}(F)$) and first ($^3A_{2g} \rightarrow {}^3T_{2g}(F)$) allowed transitions to Ni^{2+} in octahedral coordination. Coordination of Ni(II) in α-$Ni_2P_2O_7$ structure is IC = 5 and IC = 6. In other complexes with weak field oxygen ligands can be also detected five-coordinate Ni(II). Information about the Ni(II) five-coordinated ion can not be obtained from the experimental results in this study although cation coordination is obtained 5 (Ni1, Mg1) and 6 (Ni2, Mg2) in $Mg_xNi_{2-x}P_2O_7$ ($0 \le x \le 2$) solid solutions by determination of interatomic distances (Fig. 6). UV–vis–NIR spectra of these samples into glazed tiles are shown in Fig. 10. The absorption maximum of three transitions to Ni^{2+} in octahedral coordination is detected at smaller wavelength from glazed tiles than from powdered samples. It indicates modification of environment of Ni(II) ion due to instability of this structure into tested glaze.

Table 4
CIE L^* a^* b^* colour parameters in $Mg_xNi_{2-x}P_2O_7$ ($0<x<2$) samples.

x	L^*	a^*	b^*
Samples fired at 800 °C/12 h			
0.0	87.58	2.12	32.50
0.1	88.97	1.50	32.12
0.5	88.03	2.20	33.57
1.0	90.66	0.24	28.20
1.5	93.55	−0.89	19.88
2.0	98.23	−0.16	0.53
Samples fired at 1000 °C/12 h			
0.0	88.26	2.25	34.78
0.1	87.95	2.00	34.81
0.5	88.33	2.48	35.95
1.0	90.62	0.32	29.83
1.5	93.16	−0.93	22.07
2.0	97.87	−0.19	0.42
Glazed tiles from samples fired at 1000 °C/12 h			
0.0	50.98	3.96	17.95
0.1	54.64	5.72	21.39
0.5	59.21	4.33	21.81
1.0	65.90	6.98	26.65
1.5	71.73	5.76	25.09
2.0	83.87	2.10	9.50
Samples fired at 1200 °C/12 h			
0.0	76.61	7.73	45.71
0.2	78.94	7.04	44.97
0.3	77.91	9.29	46.68
0.5	79.53	8.46	45.79

CIE L^* a^* b^* parameters of $Mg_xNi_{2-x}P_2O_7$ ($0 \leq x \leq 2$) samples are shown in Table 4. The colour of these samples is yellow and the b^* parameter (yellow amount) values are similar at 800 and 1000 °C. The highest values of this parameter are obtained at 1200 °C (when Ni orthophosphate, $Ni_3(PO_4)_2$, is detected together with diphosphate solid solutions by X ray diffraction, Table 2). The b^* (+) values are obtained comparable with values obtained in others yellow materials suitable for ceramic pigments.[11] From these results, $Mg_{0.5}Ni_{1.5}P_2O_7$ composition fired at 800 °C or 1000 °C is the optimal composition to obtain yellow materials with α-diphosphate structure in conditions of this study. From this composition, best yellow colouration (maximum value of b^* parameter and value nearest to 0 of a^* parameter) is obtained in synthesis conditions of the present study.

Fig. 11 shows the UV–vis–NIR spectra in $Mg_{3-y}Ni_y(PO_4)_2$ samples fired at 300 °C and 800 °C and spectra obtained from glazed tiles (with samples fired at 800 °C). In these samples, $M_3(PO_4)_2$ (M = Ni, Mg) crystalline phase with octahedral coordination of M ion is identified from XRD when $y \neq 0$. Absorption bands detected with maximums about 430, 800 and 1300 nm are in accordance with the presence of Ni(II) ion in octahedral environment. This environment of Ni(II) ion is obtained the same from powdered samples fired at 800 °C and from glazed tiles. Shoulders observed in bands might be attributed at two crystallographic octahedral sites in $Ni_3(PO_4)_2$ structure. This fact indicates that Ni(II) orthophosphate is stable into tested glaze. More changes in Ni(II) ion environment are detected from α-diphosphate structure than from orthophosphate structure. The choice of the manufacture of materials with a structure or another one (materials with α-diphosphate structure or materials with orthophosphate structure in this case) depends on desired final industrial product.

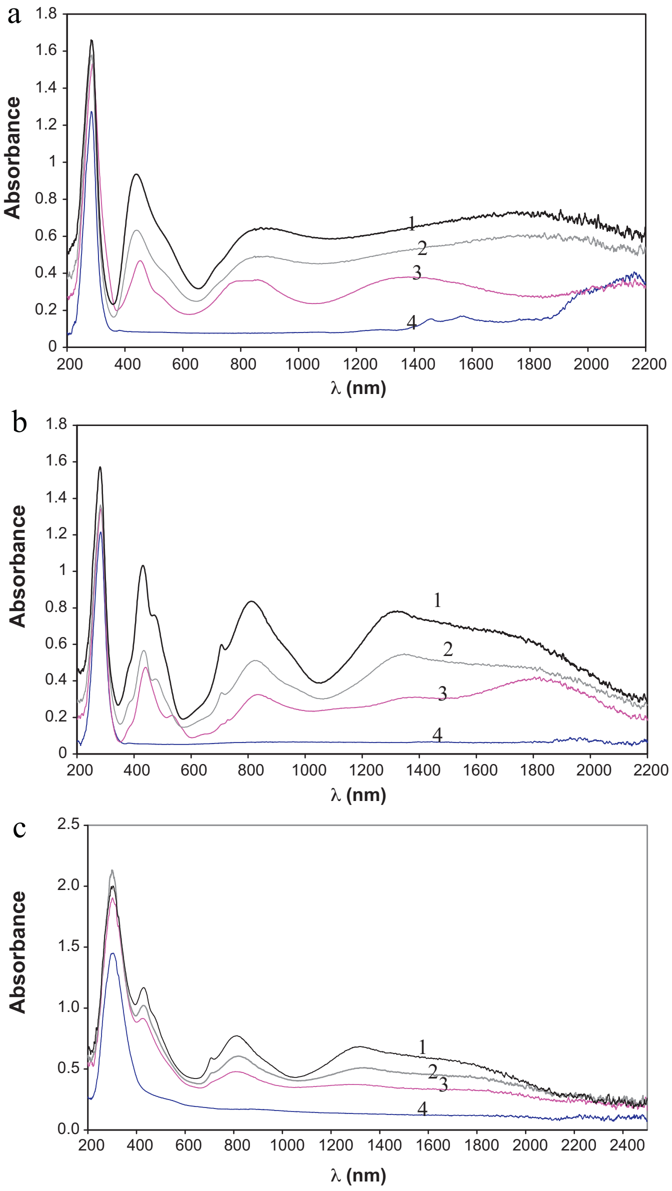

Fig. 11. UV–vis–NIR spectra of $Mg_{3-y}Ni_y(PO_4)_2$ samples with $y = 3$ (1), $y = 2$ (2), $y = 1$ (3) and $y = 0$ (4). Powdered samples fired at 300 °C/12 h (a) and 800 °C/12 h (b). Glazed tiles from samples fired at 800 °C (c).

CIE L^* a^* b^* parameters obtained from $Mg_{3-y}Ni_y(PO_4)_2$ samples fired at 800 °C are shown in Table 5. Values obtained with $Ni_3(PO_4)_2$ sample (48 wt% Ni) fired at 800 °C are comparable to these obtained with $Mg_xNi_{2-x}P_2O_7$ $0 \leq x \leq 0.5$ samples fired at 1200 °C/5 d (40–32 wt% Ni). Two-phase mixture (with α-$Ni_2P_2O_7$ and $Ni_3(PO_4)_2$ structures) are detected in these compositions fired at this temperature.

It is possible to obtain similar colourations in samples with nickel amount smaller than in $Ni_3(PO_4)_2$ or $Ni_2P_2O_7$ compounds by a thermic treatment prolonged. However cost of

Table 5
CIE L^* a^* b^* colour parameters in $Mg_{3-y}Ni_y(PO_4)_2$ $(0 \leq y \leq 3)$ samples.

Initial composition	L^*	a^*	b^*
Samples fired at 800 °C/12 h			
$y=0$: $Mg_3(PO_4)_2$	94.82	−0.34	1.47
$y=1$: $Mg_2Ni(PO_4)_2$	87.37	1.83	24.38
$y=2$: $MgNi_2(PO_4)_2$	84.44	−0.87	25.99
$y=3$: $Ni_3(PO_4)_2$	77.98	1.85	48.08
Glazed tiles from samples fired at 800 °C/12 h			
$y=0$: $Mg_3(PO_4)_2$	82.29	1.63	8.82
$y=1$: $Mg_2Ni(PO_4)_2$	67.80	5.77	28.37
$y=2$: $MgNi_2(PO_4)_2$	65.83	6.10	31.30
$y=3$: $Ni_3(PO_4)_2$	62.56	6.95	35.81

synthesis procedures and raw materials must be evaluated in ceramic industry.

4. Conclusions

Solid solutions with α-$M_2P_2O_7$ (M = Cu, Ni) and $Ni_3(PO_4)_2$ structures can be formed by the chemical coprecipitation method from $Mg_xM_{2-x}P_2O_7$ (M = Cu, $0 \leq x \leq 0.8$; M = Ni, $0 \leq x \leq 2$) and $Mg_{3-y}Ni_y(PO_4)_2$ $(1 < y \leq 3)$ compositions.

From $Mg_xCu_{2-x}P_2O_7$ compositions, the decrease of M–O (M = Mg, Cu) distances less than 3 Å might explain structural distortion and lost of stability of α-$Cu_2P_2O_7$ structure at high x values. Materials with weak greenish-blue colourations are obtained from $Mg_xCu_{2-x}P_2O_7$ $(0 \leq x \leq 2)$ compositions.

The α-$M_2P_2O_7$ (M = Ni, Mg) solid solutions are formed in all compositional range between $Ni_2P_2O_7$ and $Mg_2P_2O_7$ compounds. According with stability of this α-$Ni_2P_2O_7$ structure with composition, appreciable changes in M-O distances out of first coordination of Ni(II) or Mg(II) ions are not observed. Materials with yellow colourations are obtained from $Mg_xNi_{2-x}P_2O_7$ $(0 \leq x < 2)$ compositions.

The best yellow colouration are obtained at 1200 °C (when $Ni_3(PO_4)_2$ crystalline phase is detected together with diphosphate solid solutions). The CIE L^* a^* b^* parameters are obtained comparable with others yellow materials suitable for ceramic pigments. $Mg_{0.5}Ni_{1.5}P_2O_7$ composition fired at 800 °C or 1000 °C is the optimal composition to obtain yellow materials from α-diphosphate structure in conditions of this study. When this sample is fired at 1200 °C/5 d a diphosphate and orthophosphate mixture is obtained. Colouration obtained from this composition is comparable at that obtained from $Ni_3(PO_4)_2$ composition fired at 800 °C/12 h and nickel amount in sample is smaller in $Mg_{0.5}Ni_{1.5}P_2O_7$ composition than in $Ni_3(PO_4)_2$ composition.

Acknowledgements

M.A. Tena is grateful for the help of S. García-Granda in the present study. The author acknowledges the financial support given by the government of Spain, MAT 2008-02893 project.

References

1. Durif A. *Crystal chemistry of condensed phosphates*. New York: Plenum Press; 1995 [Chapter 2].
2. Robertson BE, Calvo C. The crystal structure and phase transformation of α-$Cu_2P_2O_7$. *Acta Cryst* 1967;**22**:665–72.
3. Calvo C. The crystal structure of α-$Mg_2P_2O_7$. *Acta Cryst* 1967;**23**:289–95.
4. Inorganic Crystal Structure Database (ICSD), Fachinformationszentrum (FIZ), Karlsruhe, Germany.
5. Meseguer S, Tena MA, Gargori C, Badenes JA, Llusar M, Monrós G. Structure and colour of cobalt ceramic pigments from phosphates. *Ceramics Int* 2007;**33**:843–9.
6. DCMA Classification and Chemical Description of the Mixed Metal Oxide Inorganic Coloured Pigments. *Metal Oxides and Ceramics Colors Subcommitee*, 2nd ed. Washington, DC: Dry Color Manufacturer's Ass.; 1982.
7. Rietveld HM. A profile refinement method for nuclear and magnetic structures. *J Appl Cryst* 1969;**2**:65–71.
8. Rodriguez-Carvajal J. Fullprof.2k computer program, version 5.00 (Jan2011-ILL-JRC), France.
9. Commission Internationale del'Eclairage. *Recommendations on Uniform Color Spaces, Color Difference Equations, Phychometrics Color Terms*, Supplement No 2 of CIE Publication No 15 (E1-1.31) 1971 (Bureau Central de la CIE, Paris, 1978).
10. Lever ABP. *Inorganic electronic spectroscopy*. 2nd ed. The Netherlands: Elsevier Science B. V; 1977. p. 507–511.
11. Sorlí S, Tena MA, Badenes JA, Calbo J, Llusar M, Monrós G. Structure and color of $Ni_xA_{1-3x}B_{2x}O_2$ (A = Ti, Sn; B = Sb, Nb) solid solutions. *J Eur Ceram Soc* 2004;**24**:2425–32.